Genomic rearrangements of the GREM1-FMN1 locus cause Oligosyndactyly, Radio-Ulnar synostosis, Hearing loss, Renal defects syndrome and Cenani-Lenz-like non-syndromic Oligosyndactyly

Boyan Ivanov Dimitrov, Thierry Voet, Luc de Smet, Joris Robert Vermeesch, Koen Devriendt, Jean-Pierre Fryns, Philippe Debeer

Genomic rearrangements of the *GREM1-FMN1* locus cause Oligosyndactyly, Radio-Ulnar synostosis, Hearing loss, Renal defects syndrome and Cenani-Lenz-like non-syndromic Oligosyndactyly

Boyan Ivanov Dimitrov[1], Thierry Voet[1], Luc De Smet[2], Joris Robert Vermeesch[1], Koen Devriendt[1], Jean-Pierre Fryns[1] and Philippe Debeer[1,2]

[1] Centre of Human Genetics, University Hospitals Leuven, Catholic University Leuven, 3000 Leuven, Belgium

[2] Department of Musculoskeletal Science, Division of Orthopedics, University Hospitals Leuven- Pellenberg, Catholic University Leuven, 3212 Pellenberg, Belgium

Address for correspondence: Prof. Dr. Philippe Debeer, Centre of Human Genetics, University Hospitals Leuven, Herestraat 49, 3000 Leuven, Belgium
Phone: +32 16 338837 or +32 16 338800
Fax: +32 16 338824
e-mail: Philippe.Debeer@uzleuven.be

Keywords: *Gremlin1*, *Formin1*, radio-ulnar synostosis, Cenani-Lenz oligosyndactyly, SHFM, limb development

Running title: *Gremlin1-Formin1* genomic rearrangements in syndromic and nonsyndromic oligosyndactyly

Word count: 2088

ABSTRACT

Limb development is a complex process requiring proper spatio-temporal expression of a network of limb specific morphogens. *Grem1* and *Fmn1* play an important role in mouse and chick limb development. The mouse *limb deformity* (*ld*) phenotype with digit reduction, syndactyly, radio-ulnar synostosis, variable renal defects and absent fibulae is caused by loss of *Grem1* function. This could be due to either coding *Grem1* homozygous mutations or homozygous deletions of the neighbouring *Fmn1* gene, which also removes limb specific regulatory sequences of *Grem1*. Recent studies reinforce the hypothesis that a loss of *Fmn1* protein could also contribute to the observed *ld* anomalies. In addition, an over-expression of *Grem1* in developing chick limbs represses the programmed cell death in the interdigital mesenchyme, resulting in interdigital webbing and truncation of distal cartilage elements.

We report here, for the first time, chromosomal imbalances in the *GREM1-FMN1* region in individuals with limb defects. A 263Kb homozygous deletion of *FMN1* was associated with oligosyndactyly, radioulnar synostosis, hearing loss and renal defects, features identical to *ld* mice. A 1.7Mb duplication encompassing both the *GREM1* and *FMN1* genes was detected in a patient with isolated Cenani-Lenz-like oligosyndactyly of the hands, resembling the transgenic chick wings in which *Grem1* was over-expressed. The phenotypes of these two patients represent new entities/syndromes within the Cenani-Lenz clinical spectrum- (1) an autosomal recessive Oligosyndactyly, Radio-Ulnar Synostosis, Hearing loss and Renal defect syndrome and (2) an autosomal dominant Cenani-Lenz-like non-syndromic Oligosyndactyly.

Vertebrate limb development serves as an important model to show how different processes and pathways are synchronized and involved in morpho- and organogenesis. As limb formation is not necessary for embryonic survival, the study of several spontaneous and molecularly manipulated (transgenic) animal models contributed to the discovery of the many genes involved in limb and skeleton patterning and development. Since several of these key genes play a role in other developmental cascades, it was also believed that this knowledge could be applied to understand the pattern formation of other tissues and organs [1, 2].

The crosstalk between two important signalling centres was found to be crucial in the complex process of limb formation - the Zone of Polarizing Activity (ZPA) and the Apical Ectodermal Ridge (AER). Key components of this mesenchymal-ectodermal (m-e) interaction are *Sonic hedgehog* (*Shh*), limb specific Fibroblast Growth Factors (FGFs) , Bone Morphogenic Proteins (BMPs) and BMP antagonists like *Gremlin 1* (*Grem1*). The study of targeted mutations of limb specific *FGF* and *BMP/ BMP* antagonist genes revealed the existence of self regulatory loops controlling the appropriate initiation and termination of m-e signalling in the coordination of limb development [3, 4, 5, 6, 7, 8]. In addition, the correct spatio-temporal expression of these limb morphogens depends on regulatory sequences surrounding the gene landscape in the vicinity [9, 10]. A good example is the *limb deformity* (*ld*) mouse. The *ld* phenotype is autosomal recessively inherited and characterized by distinct reduction defects of the digit rays, complete radioulnar synostosis, missing fibulae and variable renal defects [11]. These abnormalities are most likely a result of disturbed function of *Grem1* protein in the developing limbs due to homozygous *Grem1* mutations or loss/rearrangements of a limb bud specific *Grem1* transcriptional global controlling region (GCR) within *Fmn1* gene [9, 12, 13]. The importance of *Grem1* in limb development is further supported in that its over-expression in chick limb primordia results in truncations of distal autopod elements and syndactyly [14, 15]. Recent studies reinforce the hypothesis that a disturbed *Fmn1* protein function in limb buds may also contribute to the abnormal mouse *ld* phenotype [16].

Given the recent observation that causal submicroscopic copy number variations (CNV's) can be detected in a significant proportion of patients with unexplained congenital malformations, we analyzed seventeen individuals with either non-classified syndromic congenital skeletal anomalies or severe classified limb malformations of unknown molecular aetiology. The study was approved by the Ethics Committee of the University Hospitals Leuven. With a homemade 1Mb array Comparative Genomic Hybridization (CGH) (Supplemental data), two patients with a chromosomal rearrangement of the *GREM1-FMN1* locus on chromosome

15q13.3 were identified. In the first patient (C255625) with oligosyndactyly of the four limbs, radioulnar synostosis, hearing loss and unilateral renal aplasia (Figure 1a-d), a homozygous deletion of one BAC clone (RP11-250G15) was detected (not shown). He was previously reported as a case of Split-Hand-Foot-Malformation 1 (SHFM1) [17]. In the second patient (C80286), a two clone duplication (RP11-3D4 and RP11-250G15) encompassing the *GREM1-FMN1* locus was detected (not shown). This individual had non-syndromic Cenani-Lenz type oligosyndactyly (Figure 1e-g) [18]. No aberrations were detected in the remaining fifteen patients. For the phenotypes of the analyzed individuals and detailed reports of Patient 1 and Patient 2 with the detected microdeletion/duplication, see the Supplemental data and Supplemental table 1.

Subsequent FISH analysis (Supplemental data) using probe RP11-250G15 (red signal) confirmed the presence of a homozygous deletion in patient C255625 (Figure 2a). Several unaffected individuals from the same family were carriers of a heterozygous deletion (Figure 2a). FISH screening with probes RP11-250G15 (red signal) and RP11-3D4 (green signal) showed the *de novo* 15q13.3 tandem duplication in patient C80286 (Figure 2b).

The micro-deletion/duplication were further delineated by high resolution SNP array (Affymetrix 250K NspI, Supplemental data) in patient C255625, his parents (C359651 and C359656) and case C80286. The homozygous deletion size was maximally 263kb (between SNPs SNP_A-4201883 and SNP_A-2233558) and minimally 246kb (between SNPs SNP_A-4240484 and SNP_A-2176534), encompassing the first twelve *FMN1* exons and non-coding upstream sequences (Figure 3a-c). The healthy parents (C359651 and C359656) were heterozygous carriers of the same aberration (not shown). The duplication in patient C80286 had a maximum size of 2.3Mb (between SNP_A-2022976 and SNP_A-4217332) and a minimum size of 1.7Mb (between SNP_A-2284222 and SNP_A-2248182), including both *GREM1* and *FMN1* (Figure 3a-c). Other previously undetected CNVs, that could possibly explain the phenotype of these two affected individuals, were also excluded with the SNP array.

The quality of the SNP array CGH results was validated by RT Q-PCR (Supplemental data). Twelve primer pairs, overlapping or in the vicinity of the detected deletion/duplication breakpoints, were designed. All results were in concordance with the SNP array CGH data (not shown). One assay was used to demonstrate the *de novo* character of the microduplication in patient C80286, (Figure 3d).

To investigate the effect of these rearrangements on *GREM1* and *FMN1* expression, we studied the gene expression in the fibroblasts of both patients (Supplemental data). As a

highly variable expression pattern was observed in normal controls, a significant quantitative analysis was not possible (not shown). Of interest, in the patient C255625 with a homozygous deletion of the promoter and the first twelve *FMN1* exons, a low expression of the *FMN1* gene was detected (not shown).

The importance of the *GREM1-FMN1* locus in limb development has been extensively studied in animal models. We present for the first time evidence that this locus is implicated in human limb development. In one patient [17] a homozygous deletion of the first twelve 5' exons of the *FMN1* gene was detected. His phenotype is highly reminiscent of the *ld* mice with oligosyndactyly, radio-ulnar synostosis and renal aplasia (Figure 1a-d). The phenotypic abnormalities in this individual are similar to those of animal models in which the function of *Grem1* was abrogated, thus resulting in an abnormal m-e interaction during limb and metanephric kidney organogenesis [4, 5, 7, 8, 9, 12, 13]. In addition he has hearing loss, which has not yet been observed in the animal model. The second patient carried a *de novo* 1.7 Mb duplication encompassing the *GREM1- FMN1* locus. His isolated Cenani-Lenz-like oligosyndactyly phenotype (Figure 1e-g) [18] is similar to that of the transgenic chick in which *Grem1* over-expression causes primordial cartilage truncations and digit syndactyly due to a repression of the BMP dependant programmed cell death in the anterior necrotic zone and in the inter-digital mesenchyme. The result is a completely disorganized bone pattern of the distal autopod [14, 15].

The phenotype in *ld* mice is due to a disturbed function of the *BMP* antagonist *Grem1* either by homozygous *Grem1* mutations or a loss of *Grem1* transcriptional GCR located within the neighbouring *Fmn1* gene (Figure 4) [4, 9, 12, 13]. Therefore, the coding part of *GREM1* gene was directly sequenced in the fifteen patients in whom no causal CNVs were detected by the array CGH screening (Supplemental data). No mutations were found. In mice, the genomic region between the nineteenth and twenty-third *Fmn1* exons contains regulatory sequences controlling the *Grem1* expression in developing limbs and kidneys (Figure 4b) [9]. We determined the human homologue of this region using BLAST (blastn and bl2seq) and VISTA (genomeVISTA) alignments [19, 20]. The familial deletion of the first twelve *FMN1* exons observed in patient C255652 does not remove these regulatory sequences (Figure 4a,b). Therefore they were not included in the mutational analysis. Point mutations or undetected submicroscopic chromosomal aberrations of these or other limb specific *GREM1* regulatory sequences cannot be excluded in the fifteen individuals with negative mutation and CNV screening. There could also be a patient selection bias, since *ld* mice carrying *Grem1*

mutations have a more severe and sub-lethal phenotype [12]. Hence, the corresponding human phenotype could be different to those of our selected group [21].

In addition, the phenotype of the recently published *ld* strain is a result of a targeted deletion of *Fmn1* exon nine. This leads to a complete loss of any *Fmn1* transcript, an unexpectedly extended zone of *Grem1* expression and an increased *Bmp* activity in *ld* limb buds, indicating a direct *Fmn1* repression of the *Bmp* signalling. However the authors do not exclude the possibility that a loss of regulatory sequences could also explain the phenotype of their animal model [16]. Using computer analysis we searched for the presence of evolutionarily conserved sequences in the deleted genomic fragment in our patient. We found a few non-coding elements that could have a regulatory function and which were highly homologous through all tetrapods and chick but not present in xenopus, zebrafish and fugu [22]. Unfortunately, a direct proof of causal relationship between tissue specific regulatory sequences and their corresponding genes in humans is limited due to restrictions in obtaining appropriate patient samples for analysis (i.e. tissues in which the gene of interest is expressed at specific time points). All these findings make it difficult to judge to what extent either *GREM1* or *FMN1* contribute to the phenotype of the carrier of the homozygous 15q13.3 deletion in Family 1.

High resolution SNP array analysis of the breakpoints of the second patient (C80286) showed that low copy repeats (LCR) BP5 and BP6 on chromosome 15q13.3q14.1 flank the detected duplication. Thus the aberration is proximal to the newly recognized microdeletion 15q13.3 syndrome defined between LCR blocks BP3-BP4 and BP5 [23]. Previous studies focused on the analysis of the 15q13.3 region did not identify a similar BP5-BP6 duplication in 3699 North American controls of predominantly European ancestry [24]. Analysis of 2590 individuals in our Centre by 1Mb array CGH revealed a maternally inherited benign hemizygous deletion reciprocal to the duplication in patient C80286. Hence, there is an equal proportion of detected benign hemizygous deletions and disease causing duplications for the locus between LCR BP5-BP6. None of the few published patients with larger proximal 15q13q14 deletions encompassing the BP5-BP6 locus had distal limb anomalies [25, 26, 27].

The duplication of patient C80286 includes at least fourteen other genes besides *GREM1* and *FMN1* (Figure 3b). Currently there is no evidence in the literature that overexpression of these other genes would contribute to an abnormal limb development in humans or animal models. However, we do believe that the *de novo* character of the observed duplication in patient C80286, the absence of similar chromosomal rearrangements in a large cohort of controls screened in previous surveys [23, 24] and the strong support of an existing corresponding animal model with similar skeletal defects [14, 15] confirm the causal relationship between

the patient's phenotype and the increased copy number at the *GREM1-FMN1* locus. Since LCRs flank the detected aberration (Figure 3b), the most probable causative mechanism is non-allelic homologous recombination (NAHR) [28].

In summary, the present study delineates for the first time the human phenotype associated with a homozygous microdeletion of the *FMN1* gene. The patient's skeletal and renal defects are identical to those of *ld* mice. We also detected the human phenotype associated with a microduplication of the *GREM1-FMN1* locus in an individual with bilateral hand oligosyndactyly. No mutations of the *GREM1* gene were found among individuals with similar limb defects and/or renal anomalies. The low yield of our screening to detect genomic aberrations/point mutations in additional cases may be explained by a patient selection bias or due to restriction of the mutation analysis to the coding sequence of *GREM1*. Cenani-Lenz syndrome (CLS) was defined as a form of hand and foot syndactyly due to complete cutaneous and bony fusions. This results in disorganisation and sometimes loss of individual digit rays, and spoon-like hands. The feet are similarly affected but to a less degree. Radioulnar synostosis, mesomelic shortness, renal hypoplasia and other miscellaneous anomalies have been also observed [29]. No linkage to the *GREM1-FMN1* locus was found in a consanguineous family with offspring with classical spoon-like hands/ renal hypoplasia CLS [30]. Hence, even though our patients share some common clinical features (oligosyndactyly, radioulnar synostosis and renal abnormalities) with published CLS cases, they represent unique phenotypes caused by *GREM1*/*FMN1* alterations. Of course, genetic heterogeneity could be expected since abnormalities of genes participating or interacting with the SHH-GREM1-FMN1-FGF8/4 pathway in developing limbs, might cause identical/similar developmental defects. Therefore, our patients represent new clinical entities within the Cenani-Lenz phenotypic spectrum- (1) an autosomal recessive **Oligosyndactyly, Radio-Ulnar Synostosis, Hearing loss and Renal defect syndrome** due to a homozygous genomic deletion of *FMN1* gene, and (2) a dominant **Cenani-Lenz-like non-syndromic oligosyndactyly** caused by a duplication of *GREM1-FMN1* locus. The detected tandem 15q13.3q14 duplication delineates a new candidate for recurrent genomic disorder [33]. Analyzing more patients and further research will be necessary to unravel the clinical extent of these two new phenotypes/syndromes.

ACKNOWLEDGEMENTS

P.D. and K.D. are Clinical Research Investigators of the Fund for Scientific Research, Flanders, Belgium. B.D. was partially supported by grant EO/06/32 of the Catholic University of Leuven, Belgium.

Competing Interest: None to declare.

Figure 1. Clinical phenotype of patients C255625 and C80286. Patient C255625 was published as an atypical case of SHFM1 (20). There is bilateral oligosyndactyly with four fingers on the right hand (1a) and three on the left (1b). The nails of the digits are normal. Both feet have an absent second ray and four remaining toes. (1c). An excretory contrast X-ray examination demonstrates agenesis of the left kidney (1d). The phenotype of patient C80286 was previously classified as an isolated Cenani-Lenz-like oligosyndactyly of all fingers of both hands (21). Radiographs of the hands at 6 months of age (1e) and at 27 years of age (1f) show progressive multiple fusions of metacarpal bones and phalanges with several missing skeletal elements. Fusion of carpal bones is also present. Both feet have no skeletal anomalies (1g). Appropriate informed consent was obtained from the participating patients or their legal representatives.

Figure 2. Pedigrees of patient C255625 (Family 1) and patient C80286 (Family 2). Below each individual partial metaphase spreads or interphase nuclei are shown summarizing the results of the performed FISH analysis. Filed red and green colour squares represent the patients. Striped red circles and squares show heterozygous carriers in Family 1. A) BAC RP11-250G15 (red signal), with genomic position as shown on Figure 3c, was used as a FISH probe to confirm the abnormalities detected by the array CGH screening in Family 1. A chromosome 15q subtelomeric probe (green signal) served as a control. Arrows point to the aberrant alleles (with deletion) in the analyzed individuals. There was no hybridization of BAC RP11-250G15 (red signal) on both chromosomes 15 in patient C255625. This is in correlation with the array CGH results and demonstrates that the patient has a homozygous deletion of the genomic locus covered by this probe. FISH analysis showed a hybridization of BAC RP11-250G15 (red signal) on only one metaphase chromosome fifteen in heterozygous carriers of the aberration in Family 1, the parents (C359656 and C359651) and two additional siblings (C367866 and C367867) respectively. In addition, a cross-hybridization of BAC RP11-250G15 (red signal) on chromosome 3q was also observed in all analyzed metaphases. B) To confirm the presence of the microduplication in patient C80286, FISH analysis was done on interphase nuclei using two FISH probes residing within the aberration, BAC RP11-250G15 (red signal) and BAC RP11-3D4 (green signal). All patient's nuclei had one pair of a red and a green signal representing the normal allele, and a string of two red and two green signals corresponding to the allele carrying the duplication. Arrow points the aberrant allele (with duplication). The linear order of these four signals was always red-green-red-green suggesting a tandem orientation of the duplicated fragments. Both parents (C80284 and

C80285) were not carriers of the aberration. In addition, all analyzed patient's and parental nuclei presented two more red signals. These two additional signals were every time separated from the others and were not paired with green one, demonstrating a cross-hybridization of BAC RP11-250G15 on chromosome 3q. Subsequently, this cross-hybridization was also confirmed on parental and patient's chromosomal metaphase spreads (not shown). Appropriate informed consent was obtained from the participating patients or their legal representatives.

Figure 3. *GREM1-FMN1* locus on chromosome 15q13.3 and genomic positions of the detected homozygous deletion (C255625) and *de novo* duplication (C80286) according the Human Reference Sequence March 2006, NCBI Build 36.1. A) Fine mapping of the breakpoints by 250 NspI SNP array of Affymetrix in patient C255625 and C80286. B) Genomic architecture of the aberrant locus. Transparent vertical green and pink lines demarcate the positions of the breakpoints. Low copy repeats (BP5 and BP6) flank the detected *de novo* 1.7Mb (minimal size) tandem duplication (dark green bar) of patient C80286. C) Colour bars and triangles show the positions of the used BACs as FISH probes and some of the RT Q-PCR primers. Dark red and green bars represent the homozygous deletion (minimal size) of C255625 and the tandem *de novo* duplication (minimal size) of C80286, respectively. D) Results of the RT Q-PCR with five of the primers used to confirm the SNP array CGH results and their corresponding genomic locations according the detected chromosomal aberrations in Family 1 and Family 2 (Supplemental table 1). The bars visualize the present relative allele copy number (fold differences). Value of 1 stands for the normal diploid status, 0.5 is for hemizigousity, 0 for homozygous deletion and 1.5 for a duplication, respectively. The closest outside primers flanking the breakpoints of the detected homozygous deletion in case C255625 (Family 1) are shown in blue (Pr5) and yellow (Pr10) colours. The red (Pr6) and pink (Pr9) bars represent the closest inside primers to the breakpoints of the same patient. The green bar demonstrates the primer (Pr7) used for detection of the parental origin of the duplication in case C80286 (Family 2). Both parents (C80284 and C80285) have a normal diploid allele copy number. Appropriate informed consent was obtained from the participating patients or their legal representatives.

Figure 4. Alignment of the human and mouse *GREM1-FMN1* locus. A) The human *GREM1-FMN1* locus (Human Reference Sequence March 2006, NCBI Build 36.1) and the detected in Family 1 deletion (transparent pink bar). B) The mouse *Grem1* and *Fmn1* genomic position

and structure [9] (Build 37 assembly by NCBI and the Mouse Genome Sequencing Consortium, July 2007). All known mouse mutations mapped to this landscape are indicated above or below the *Grem1-Fmn1* genomic structure. Δ*4,* Δ*5,* Δ*6,* Δ*9,* Δ*10-24, ldOR* and *Grem1*Δ are targeted deletions. Point mutations (*ldJ*), inversions (*ldIn2*) and transgenic insertions (*ldTgBri, ldTgHd)* are also shown. Mutations marked in red cause the *ld* phenotype in mice (modified from reference 10). Transparent pink bars highlight the detected 246Kb (minimal size) deletion of patient C255625.

REFERENCES

1. Niswander, L. Pattern formation: old models out on a limb. *Nat Rev Genet* 2003;4:133-143.
2. Tickle, C. Making digit patterns in the vertebrate limb. *Nat Rev Mol Cell Biol* 2006;7:45-53.
3. Zuniga, A., Haramis, A.P., McMahon, A.P., Zeller, R. Signal relay by BMP antagonism controls the *SHH*/*FGF4* feedback loop in vertebrate limb buds. *Nature* 1999;401:598-602.
4. Khokha, M.K., Hsu, D., Brunet, L.J., Dionne, M.S., Harland, R.M. Gremlin is the BMP antagonist required for maintenance of *Shh* and *Fgf* signals during limb patterning. *Nat Genet* 2003;34:303-307.
5. Scherz, P.J., Harfe, B.D., McMahon, A.P., Tabin, C.J. The limb bud Shh-Fgf feedback loop is terminated by expansion of former ZPA cells. *Science* 2004;305: 396-399.
6. Mariani, F.V., Ahn, C.P., Martin, GR. Genetic evidence that FGFs have an instructive role in limb proximal-distal patterning. *Nature* 2008;453:401-405.
7. Verheyden, J.M., Sun, X. An *Fgf*/*Gremlin* inhibitory feedback loop triggers termination of limb bud outgrowth. *Nature* 2008;454:638-641.
8. Bénazet, J.D., Bischofberger, M., Tiecke, E., Gonçalves, A., Martin, J.F., Zuniga, A., Naef, F., Zeller, R. A self-regulatory system of interlinked signaling feedback loops controls mouse limb patterning. *Science* 2009;323:1050-1053.
9. Zuniga, A., Michos, O., Spitz, F., Haramis, A.P., Panman, L., Galli, A., Vintersten, K., Klasen, C., Mansfield, W., Kuc, S., et al. Mouse *limb deformity* mutations disrupt a global control region within the large regulatory landscape required for *Gremlin* expression. *Genes Dev* 2004;18:1553-1564.
10. Zeller, R., Zuniga, A. *Shh* and *Gremlin1* chromosomal landscapes in development and disease. *Curr Opin Genet Dev* 2007;17:428-434.
11. Kleinebrecht, J., Selow, J., Winkler, W. The mouse mutant *limb-deformity* (*ld*). *Anat Anz* 1982;152:313-324.
12. Michos, O., Panman, L., Vintersten, K., Beier, K., Zeller, R., Zuniga, A. *Gremlin*-mediated *BMP* antagonism induces the epithelial-mesenchymal feedback signaling controlling metanephric kidney and limb organogenesis. *Development* 2004;131:3401-3410.

13. Pavel, E., Zhao, W., Powell, K.A., Weinstein, M., Kirschner, L.S. Analysis of a new allele of *limb deformity* (*ld*) reveals tissue- and age-specific transcriptional effects of the Ld Global Control Region. *Int J Dev Biol* 2007;51:273-281.
14. Capdevila, J., Tsukui, T., Rodríquez Esteban, C., Zappavigna, V., Izpisúa Belmonte, J.C.. Control of vertebrate limb outgrowth by the proximal factor *Meis2* and distal antagonism of BMPs by *Gremlin*. *Mol Cell* 1999;4:839-849.
15. Merino, R., Rodriguez-Leon, J., Macias, D., Gañan, Y., Economides, A.N., Hurle, J.M. The *BMP* antagonist *Gremlin* regulates outgrowth, chondrogenesis and programmed cell death in the developing limb. *Development* 1999;126:5515-5522.
16. Zhou, F., Leder, P., Zuniga, A., Dettenhofer, M. *Formin1* disruption confers oligodactylism and alters *Bmp* signaling. *Hum Mol Genet* 2009;18:2472-2482.
17. Debeer, P., Vandenbossche, L., de Ravel, T.J., Desloovere, C., De Smet, L., Huysmans, C., Thoelen, R., Vermeesch, J., Van de Ven, W.J., Fryns, J.P. Bilateral complete radioulnar synostosis associated with ectrodactyly and sensorineural hearing loss: a variant of SHFM1. *Clin Genet* 2004;65:153-155.
18. De Smet, L., Winnepenninckx, B., Fryns, J.P., Fabry, G. Cenani-Lenz type of syndactyly: a complex type of syndactyly with multiple synostoses. *Genet Couns* 1992;3:145-147.
19. McGinnis, S., Madden, T.L. BLAST: at the core of a powerful and diverse set of sequence analysis tools. *Nucleic Acids Res* 2004;32:W20-W25.
20. Frazer, K.A., Pachter, L., Poliakov, A., Rubin, E.M., Dubchak, I. VISTA: computational tools for comparative genomics. *Nucleic Acids Res* 2004;32:W273-W279.
21. Kleinjan, D.A., Lettice, L.A. Long-range gene control and genetic disease. *Adv Genet* 2008;61:339-388.
22. Loots, G. Genomic identification of regulatory elements by evolutionary sequence comparison and functional analysis. *Adv Genet* 2008;61:269-293.
23. Sharp, A.J., Mefford, H.C., Li, K., Baker, C., Skinner, C., Stevenson, R.E., Schroer, R.J., Novara, F., De Gregori, M., Ciccone, R., et al. A recurrent 15q13.3 microdeletion syndrome associated with mental retardation and seizures. *Nat Genet* 2008;40:322-328.
24. Helbig I., Mefford H.C., Sharp A.J., Guipponi M., Fichera M., Franke A., Muhle H., de Kovel C., Baker C., von Spiczak S., et al. 15q13.3 microdeletions increase risk of idiopathic generalized epilepsy. *Nat Genet* 2009;41:160-162.

25. Matsumura, M., Kubota, T., Hidaka, E., Wakui, K., Kadowaki, S., Ueta, I., Shimizu, T., Ueno, I., Yamauchi, K., Herzing, L.B., et al. 'Severe' Prader-Willi syndrome with a large deletion of chromosome 15 due to an unbalanced t(15,22)(q14;q11.2) translocation. *Clin Genet* 2003;63:79-81.
26. Windpassinger, C., Petek, E., Wagner, K., Langmann, A., Buiting, K., Kroisel, P.M. Molecular characterization of a unique de novo 15q deletion associated with Prader-Willi syndrome and central visual impairment. *Clin Genet* 2003;63:297-302.
27. Erdogan, F., Ullmann, R., Chen, W., Schubert, M., Adolph, S., Hultschig, C., Kalscheuer, V., Ropers, H.H., Spaich, C., Tzschach, A. Characterization of a 5.3 Mb deletion in 15q14 by comparative genomic hybridization using a whole genome "tiling path" BAC array in a girl with heart defect, cleft palate, and developmental delay. *Am J Med Genet A* 2007;143:172-178.
28. Gu, W., Zhang, F., Lupski, J.R. Mechanisms for human genomic rearrangements. *PathoGenetics* 2008;1:4.
29. Harpf, C., Pavelka, M., Hussl, H. A variant of Cenani-Lenz syndactyly (CLS): review of the literature and attempt of classification. *Br J Plast Surg* 2005;58:251-257.
30. Bacchelli C., Goodman F.R., Scambler P.J., Winter R.M. Cenani-Lenz syndrome with renal hypoplasia is not linked to *FORMIN* or *GREMLIN*. *Clin Genet* 2001;59:203-205.

Figure 1

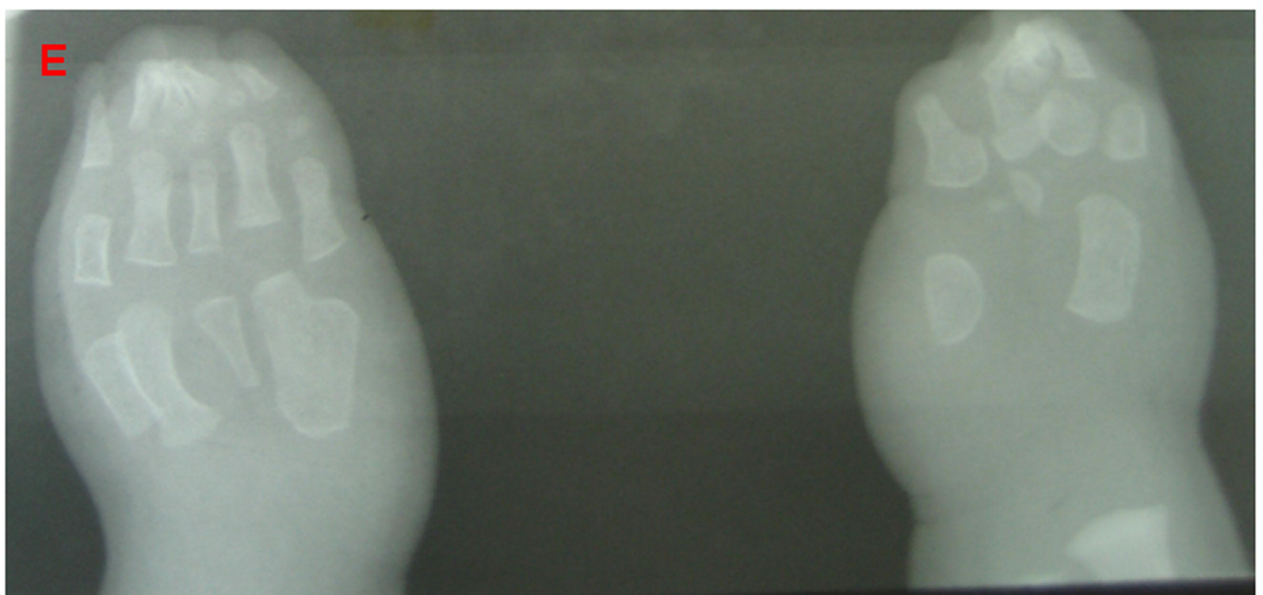

Figure 2

A)

Family 1

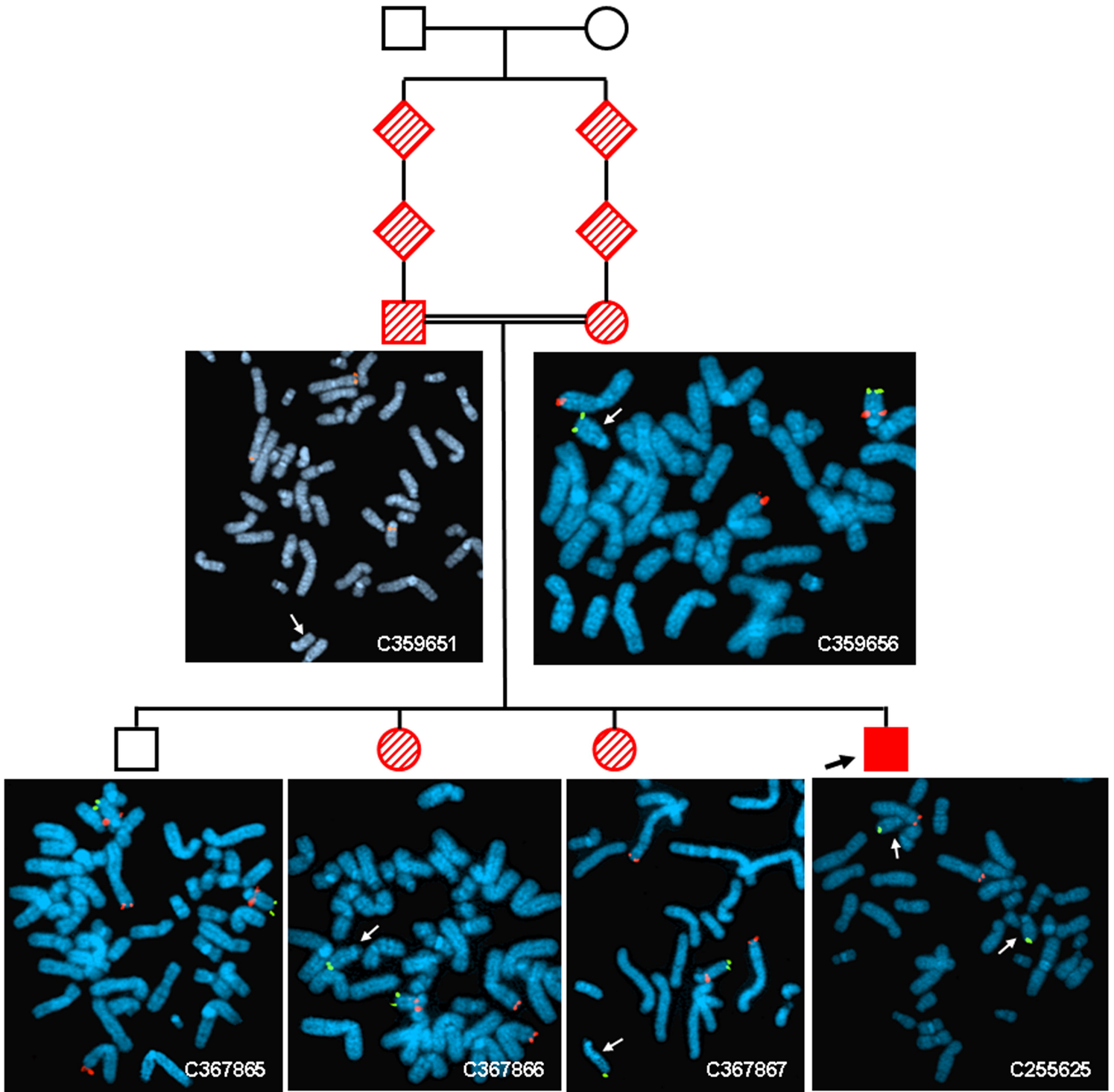

B)

Family 2

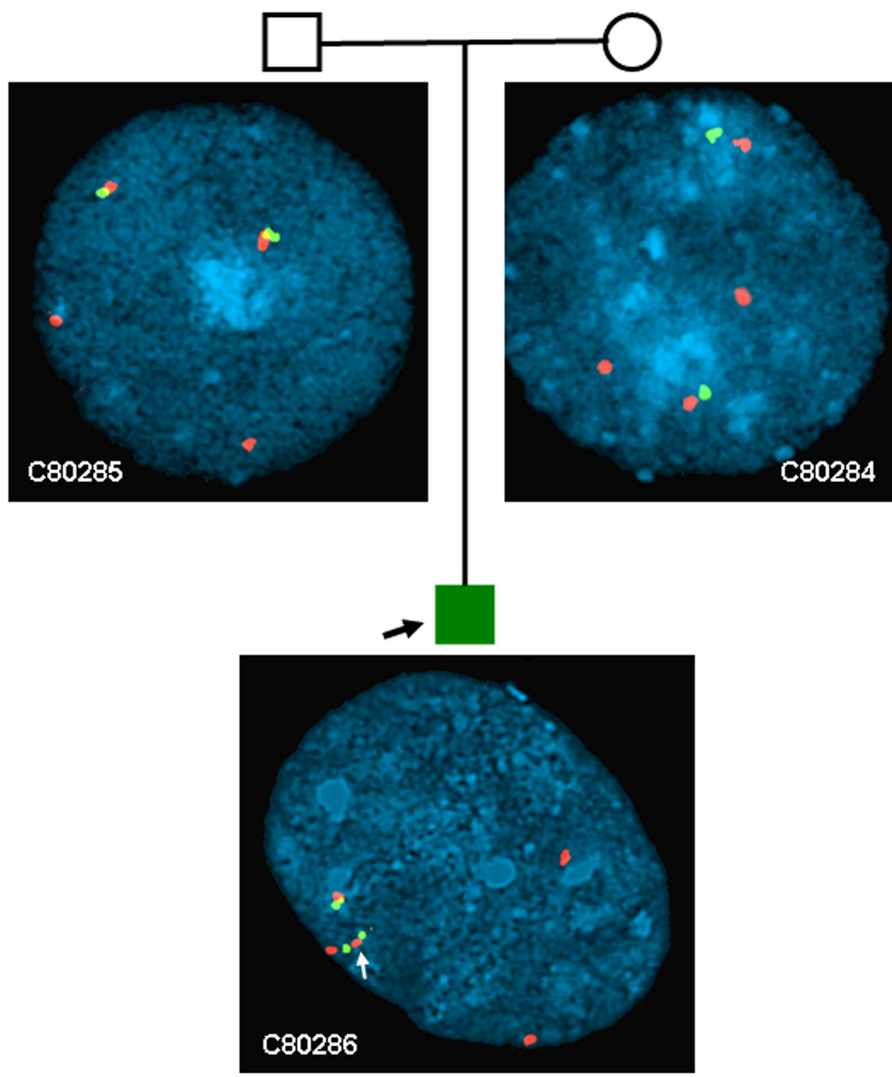

Figure 3

A)

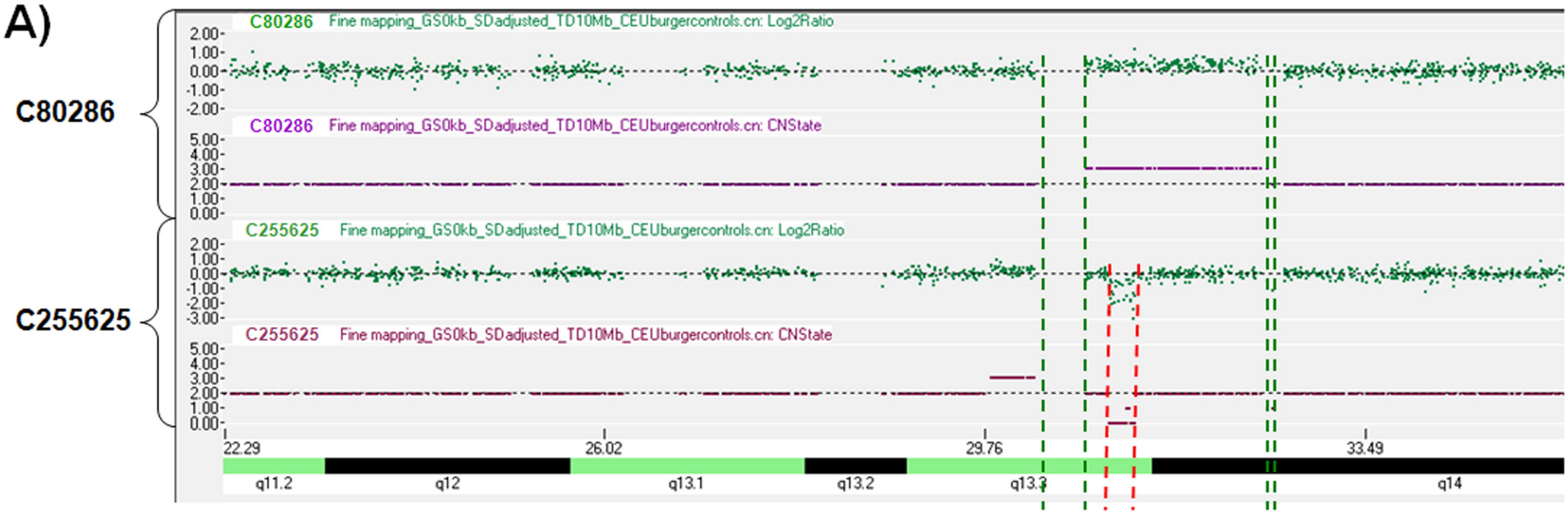

B)

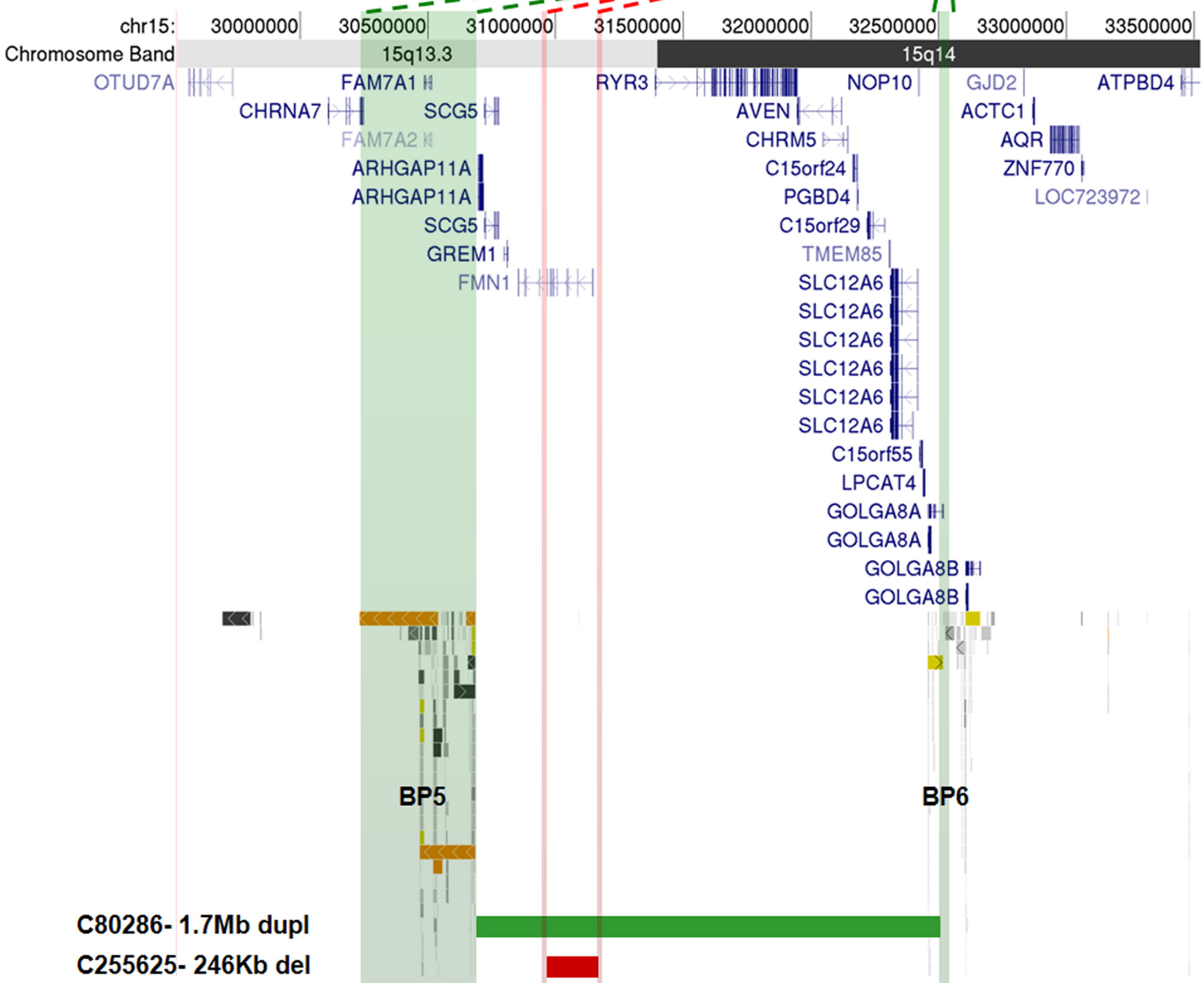

C)

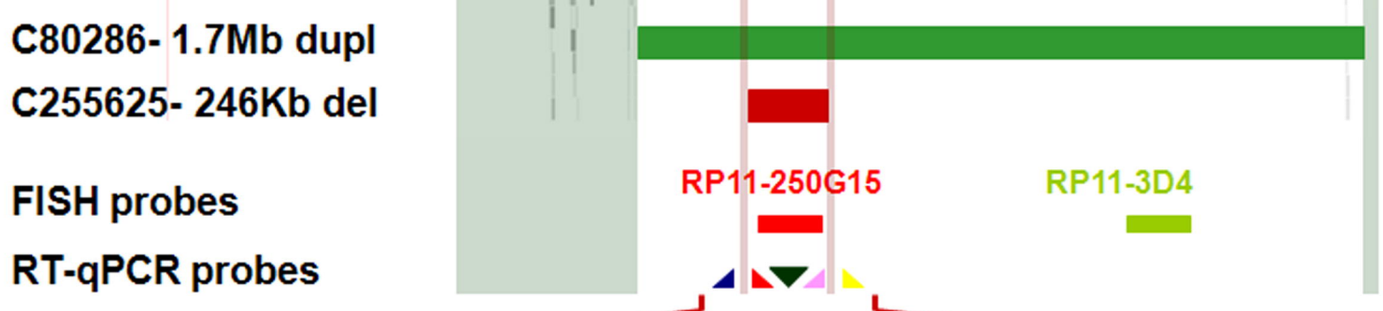

D)

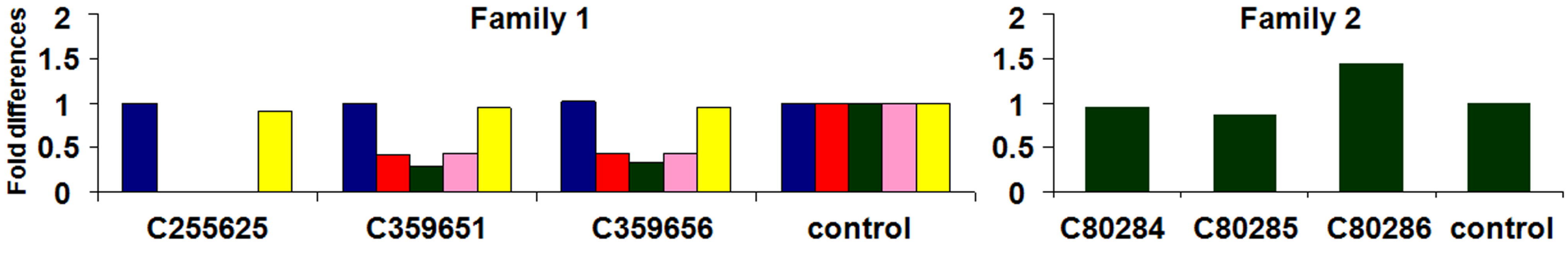

Figure 4

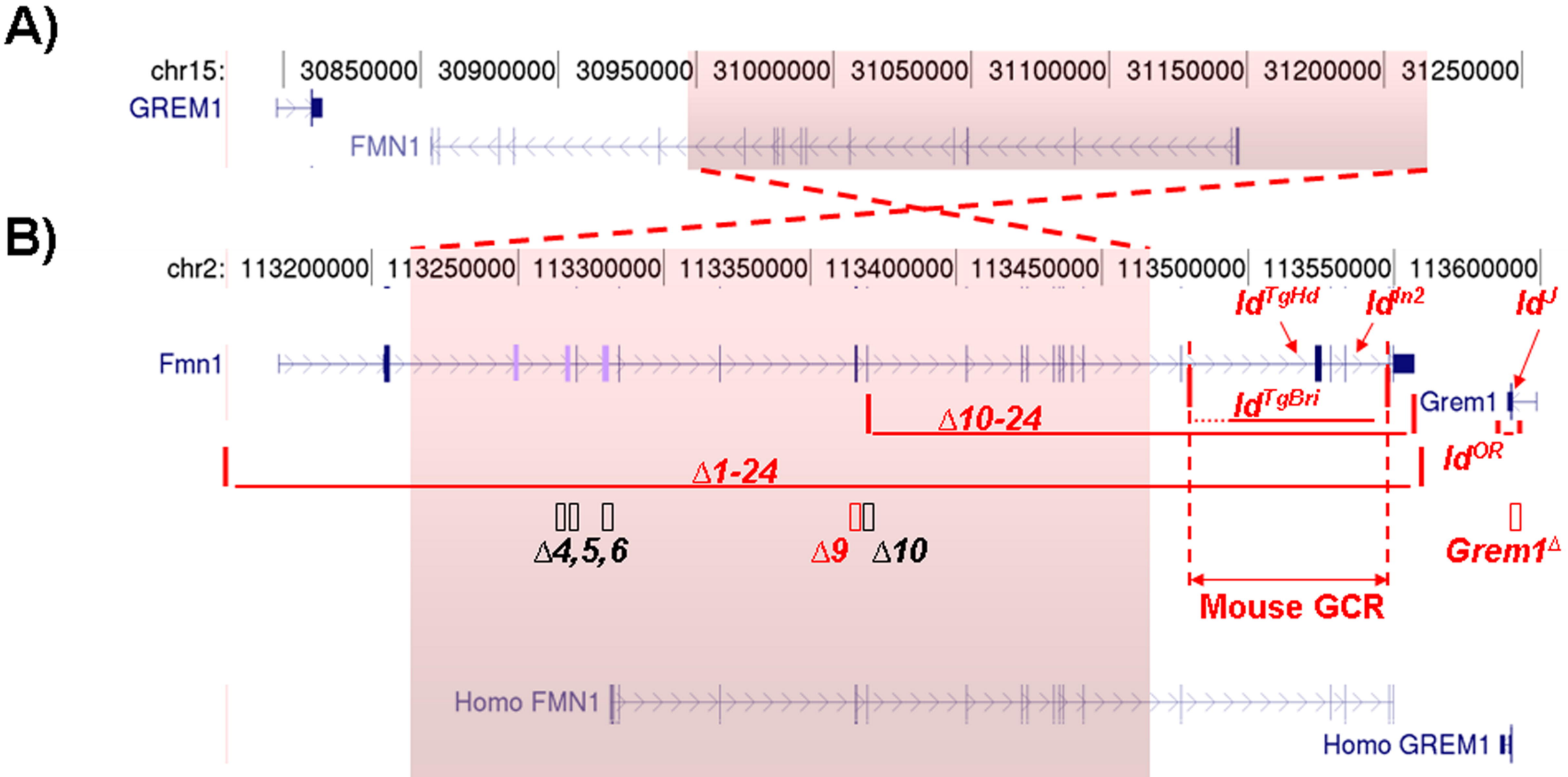
A)
chr15:
30850000
30900000
30950000
31000000
31050000
31100000
31150000
31200000
31250000
GREM1
FMN1
B)
chr2:
113200000
113250000
113300000
113350000
113400000
113450000
113500000
113550000
113600000
Fmn1
Id^TgHd
Id^In2
Id^J
Id^TgBri
Grem1
Δ10-24
Id^OR
Δ1-24
Δ4,5,6
Δ9
Δ10
Grem1^Δ
Mouse GCR
Homo FMN1
Homo GREM1